Title	Development of muon spin imaging spectroscopy
Author(s)	Sugisaki, Takato; Kojima, Kenji M.; Mihara, Mototsugu et al.
Citation	Interactions. 2024, 245(1), p. 32
Version Type	AO
URL	https://hdl.handle.net/11094/102642
rights	
Note	

Development of Muon Spin Imaging Spectroscopy

Takato Sugisaki[1,2,8,9*], Kenji M. Kojima[2,8*], Mototsugu Mihara[1,8*], Yoko Kimura[1,8], Yutaka Mizoi[3,8], Gen Takayama[1], Daiki Nishimura[4], Masaomi Tanaka[5,8], Soshi Ishitani[1], Gerald Morris[2], Donald Arseneau[2], Rahim Abasalti[2], Deepak Vyas[2], Mitsunori Fukuda[1], Wataru Sato[6], Runa Yasuda[7], Ryo Taguchi[1]

[1]Department of Physics, Osaka University, 1-1 Machikaneyama-cho, Toyonaka-shi, 560-0043, Osaka, Japan.
[2]CMMS, TRIUMF, 4004 Wesbrook Mall, Vancouver, V6T 2A3, BC, Canada.
[3]Osaka Electro-Communication University, 18-8 Hatsu-cho, Neyagawa-shi, 572-8530, Osaka, Japan.
[4]Tokyo City University, 1-28-1 Tamazutsumi, Setagaya-ku, 158-8557, Tokyo, Japan.
[5]Faculty of Arts and Science, Kyushu University, Nishi-ku, Fukuoka-shi, 819-0395, Fukuoka, Japan.
[6]Kanazawa University, Kakuma-machi, Kanazawa-shi, 920-1192, Ishikawa, Japan.
[7]Tokyo University of Agriculture and Technology, 2-24-16 Naka-cho, Koganei-shi, 184-8588, Tokyo, Japan.
[8]Open-it, http://openit.kek.jp.
[9]IMSS, KEK, 203-1 Shirakata, Tokai-mura, Naka-gun, 319-1106, Ibaraki, Japan.

*Corresponding author(s). E-mail(s): sugisaki@ne.phys.sci.osaka-u.ac.jp; kojima@triumf.ca; mihara@vg.phys.sci.osaka-u.ac.jp;

Abstract

Muon spin relaxation/rotation/resonance (μ**SR**) method is one of the most effective experimental methods and has been used in many fields such as material science, chemical, and bioscience since the 1970s. For the next elevation of μ**SR**, we developed positron detectors that have a spatial resolution and used them as positron trackers so that we could construct an image of a sample. Demonstrative experiments of trackers were performed at TRIUMF and an image of a sample was successfully reconstructed.

Keywords: μSR, Imaging, Plastic scintillation fiber, Positron tracking

1 Introduction

The muon spin relaxation/rotation/resonance (μSR) technique that provides information on the local magnetic field inside materials has been widely applied to a variety of scientific and industrial research [1]. However, in conventional μSR measurements, only the information about the overall sample can be extracted because the detector set does not have any spatial resolutions. If it becomes possible to acquire μSR spectra for each position in the sample, it will enable us to extract and construct images of specific properties of materials, as it is widely used in the magnetic resonance imaging (MRI).

An attempt to make such an image as those observed in μSR spectroscopy has been reported previously on the development of "muon spin imaging", named by N. Kaplan et al. [2]. In order to obtain information about where μ^+ stops in the sample, they applied a magnetic field gradient to the sample. In contrast, we developed a new positron tracking detector set that has a spatial resolution instead. This allows imaging without scanning the beam or applying a magnetic field gradient to the sample.

We performed experiments using μ^+ beams to demonstrate this new detector. μSR spectra at each position of a test sample were extracted by positron tracking, from which we attempted to create an image.

2 Positron Trackers for Muon Spin Imaging Spectroscopy

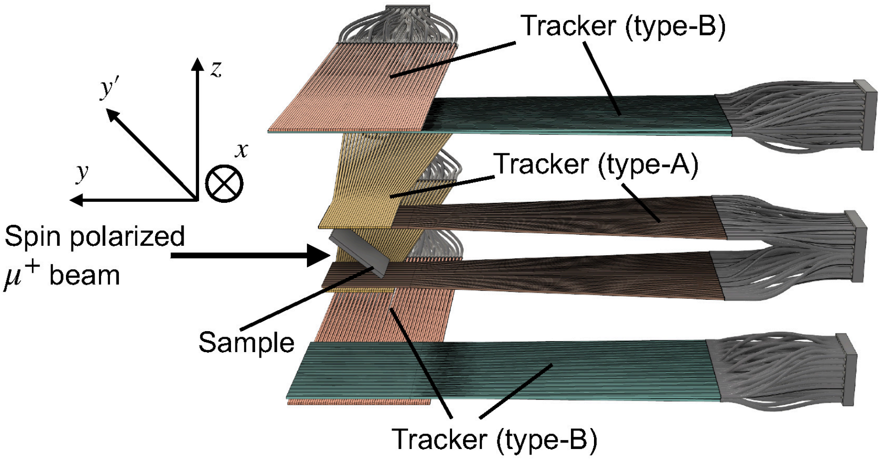

Fig. 1: Image of all the trackers setup

In order to realize the muon spin imaging, we have developed the following new positron (e^+) detector system that can be integrated into the μSR spectrometer. This system we named "fiber trackers" shown in Fig. 1, is made of plastic scintillating fibers (PSFs) [3], optical fibers, and Multi-Pixel Photon Counter (MPPC) arrays [4]. They are the exactly same as the one used in "$\beta -$MRI" study [5][6]. The photos of the trackers are shown in Fig. 2. The trackers consist of two sets of a counter telescope placed above (UP) and below (DOWN) the sample. Each telescope has two layers of two dimensional (2D) positron sensitive detectors consisting of two pairs of 1 mm square PSFs arranged in a planar configuration and stacked orthogonally to each other. The number of PSFs is 32×32 and 64×64 for the inner and outer layers, respectively. As shown in Fig 1 and 2, there are two types of trackers, type-A for inner layers and type-B for outer layers.

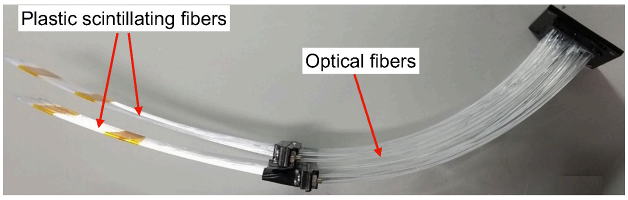

(a) Type-A; A tracker used for two inner layers (see text)

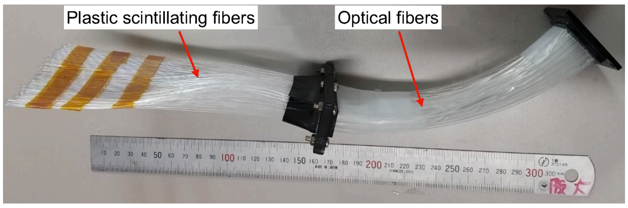

(b) Type-B; A tracker used for an outer layer (see text)

Fig. 2: Photos of trackers before being shaded

These trackers enable us to track e^+ back and then to determine its source position, which is the original position of the parent particle of μ^+ in the sample. Figure 3 shows how to extract a source position. As the μ^+ beam used for the experiments was "surface muon beam", so the momentum was 29.8 MeV/c and the stopping range of μ^+ by the sample was less than 1 mm, the sample can be regarded as a plane. In the present experiments, the sample was tilted by 45° relative to the $x - z$ plane, so the plane, where μ^+ stopped, could be represented as $z = y$. Therefore, the source position can be extracted from the intersection of this plane and the straight line determined by two hit positions. Details on how to create images using the positron tracking are discussed in [7].

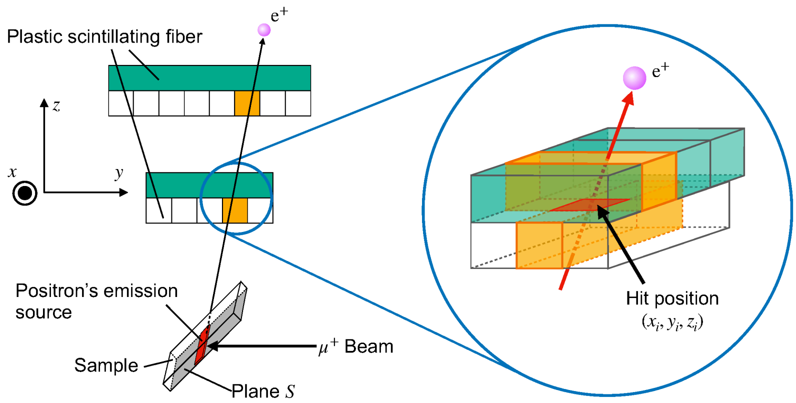

Fig. 3: How to find the coordinate that e^+ passes through the inner layer. The coordinate on the outer layer is also determined in the same way. From these two coordinates, a straight line along the trajectory can be sought. Plane S corresponds to the surface of the sample where μ^+ stops. Source position is determined by the intersection of S and the straight line

3 Experiment

Experiments were performed at M20C beamline [8] at TRIUMF in Canada [9] using μ^+ beams with conditions summarized in Table 1. The schematic view and photo of the experimental setup are shown in Fig. 4. All the trackers and the sample were fixed with an acrylic supporting frame placed at the end of the beamline. In addition, a total of five plastic scintillation counters were installed: one was set upstream of the sample to obtain timing signals of incident μ^+, and the other two sets of counters were installed above and below the trackers to detect positrons, generating trigger signals by coincidence events with the trackers.

A static magnetic field of ∼11 G was applied to the sample perpendicular to the beam axis by a Helmholtz coil to observe the transverse field muon spin rotation (TF-μSR).

Table 1: μ^+ beam conditions

Momentum	Energy	Polarization	Intensity	Beam Size
29.8 MeV/c	4.12 MeV	∼100%	∼ 800 muons/s	Circle 20 mm in diameter

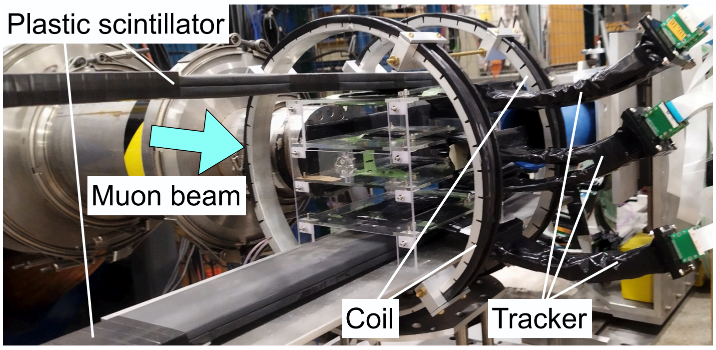

(a) Photo of the experimental setup

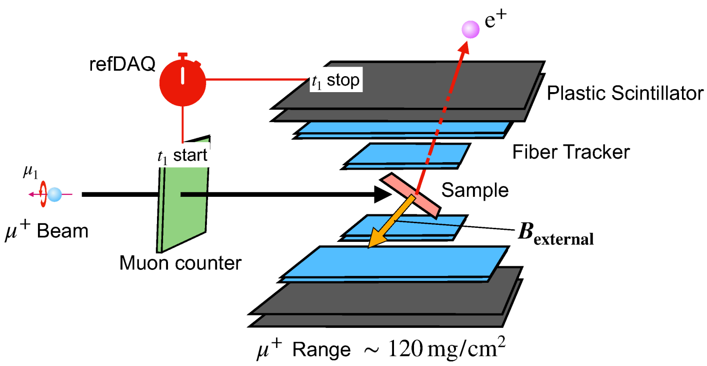

(b) Schematic view of the experimental setup

Fig. 4: Photo snd schematic view of the experimental setup

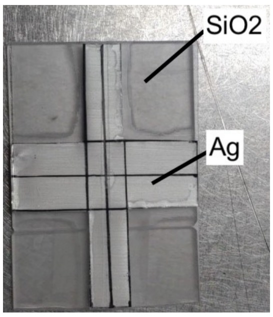

(a) Photo of Ag+SiO_2 sample

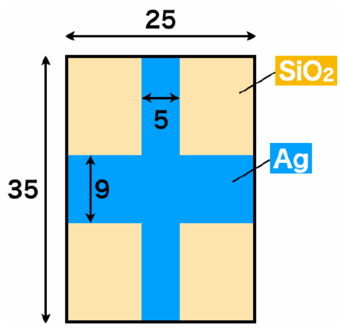

(b) Drawing of Ag+SiO_2 sample

Fig. 5: Photo and drawing of Ag+SiO_2 sample

In order to demonstrate the muon spin imaging by our new system, we prepared a "Ag+SiO_2" sample shown in Fig. 5.

The reason why we prepared this sample is the μSR time spectra in Ag and SiO_2 are known to be quite different. In Ag, μ^+ exists as it is i.e. in a diamagnetic Mu^+ state, whereas μ^+ in SiO_2 mainly picks an electron up and forms a paramagnetic muonium state described as Mu^0 [10]. Under the weak magnetic field limit, the gyromagnetic ratios of Mu^+ and Mu^0 are the following respectively.

$$\frac{\gamma_{\mathrm{Mu}^+}}{2\pi} = 0.13\,\mathrm{MHz/G} \tag{1}$$

$$\frac{\gamma_{\mathrm{Mu}^0}}{2\pi} = 1.4\,\mathrm{MHz/G} \tag{2}$$

The Mu^0 spin precesses about 100 times faster than Mu^+ spin. Therefore, we can distinguish Ag and SiO_2 by observing weak TF-μSR time spectra at each position in the mixed sample.

4 Result

The data obtained in the present study were analyzed using the analysis tool "ROOT" [11]. Firstly, a μ^+ beam profile was obtained by tracking positrons as shown in Fig. 6. The sample edges and material boundaries expected from this profile are also shown in the same figure. Here, sufficient statistics were not obtained to divide the area into small pixels. Therefore, we divided the profile into nine parts (00–08) based on the expected boundaries.

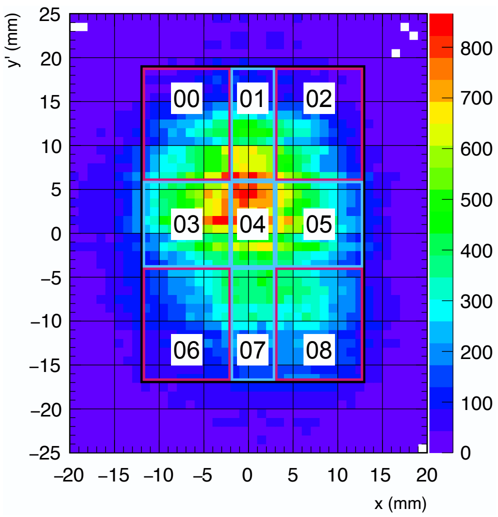

Fig. 6: Divided the profile obtained by tracking positrons of Ag+SiO_2 sample

Then, asymmetry $A(t)$ for each area was deduced with Eq. (3), which is shown in Fig. 7.

$$A^i(t) = \frac{N_U^i(t) - N_D^i(t)}{N_U^i(t) + N_D^i(t)} \tag{3}$$

Also, Fig. 8 shows the visualized amplitudes of nine μSR time spectra for each area.

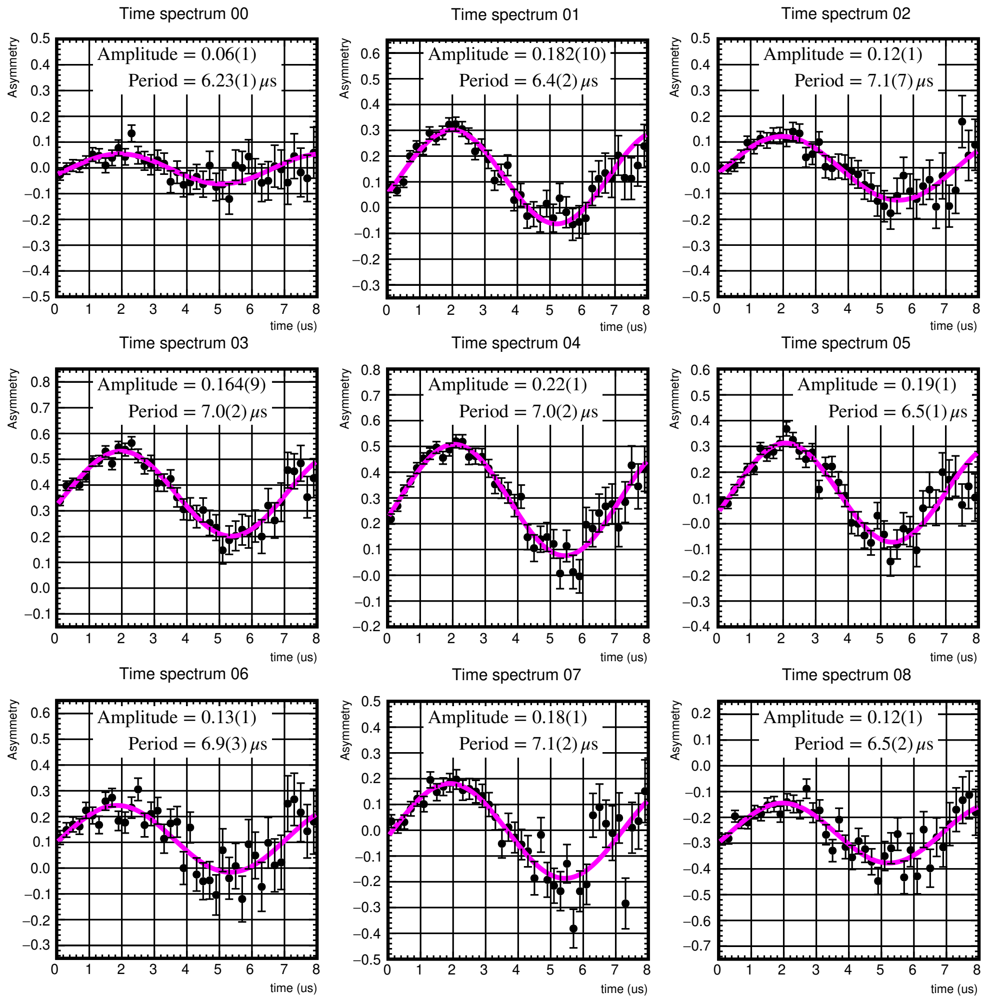

Fig. 7: Time spectrum of asymmetry$A(t)$ for each area. Numbers on the title of each spectrum correspond to the ones in Fig. 6. Amplitudes $A(0)$ and periods $T = 2\pi/\omega$ from Eq. (4) are mentioned on all the time spectra

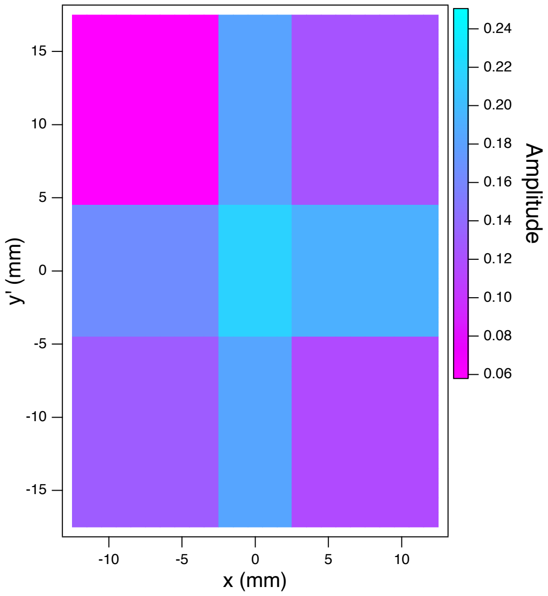

Fig. 8: Visualized amplitudes of μSR time spectra at nine areas of Ag+SiO_2 sample

All the time spectra are fitted with the following function $f(t)$:

$$f(t) = A(0) \sin \{\omega (t - x_0)\} + C, \tag{4}$$

where $A(0)$, ω, x_0, C are all parameters for this fitting function. As seen in Fig. 7, the amplitudes for the center and all the adjacent areas tend to be larger than those for the four corner areas. Note that the width of the time bins in these spectra are so large that the fast Mu^0 spin rotation is buried and only the slow Mu^+ spin rotation with the period $\sim 7\,\mu s$ is visible. So, this tendency seems reasonable because the amplitudes of the slow rotation appear to reflect the configuration of materials.

To make sure that Mu^0 were really formed in SiO_2, we considered the integration of four data in the 00, 02, 06, and 08 areas and that of the rest 5 areas and focused our eyes on 0–2 µs because the precession of Mu^0 is quite rapid, which is estimated to be $\nu_{Mu^0} = 14\,MHz$

After the integration, we performed Fast Fourier Transform (FFT) to the two integrated μSR time spectra with the time bin width set at 0.025 µs in order to extract frequency components.

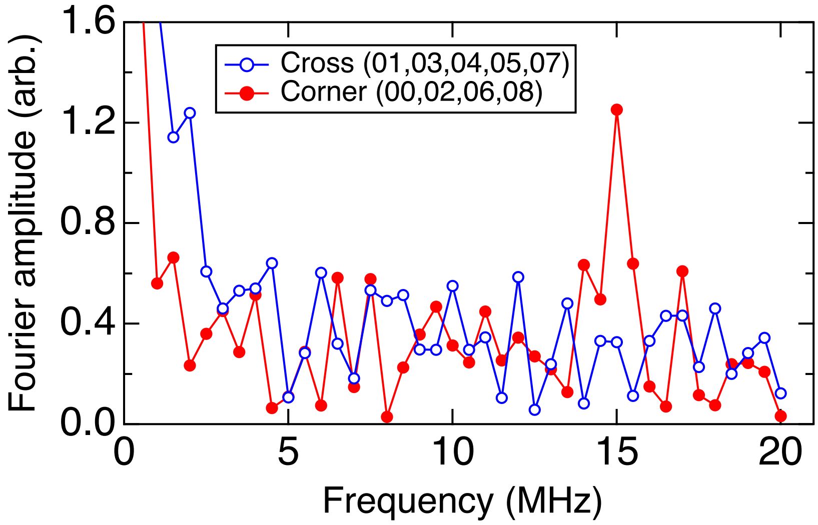

Fig. 9: Result of FFT. The red solid circle indicates the FFT spectrum of integrated TF-μSR spectra in the corner (00, 02, 06, and 08) areas. The blue open circle indicates the one in the cross (01, 03, 04, 05, and 07) areas.

As the result is shown in Fig. 9, the frequency around 15 MHz is observed only for SiO_2, which is almost consistent with the expected value of ν_{Mu^0}. Considering that there are no other remarkable peaks around it for Ag, this strongly suggests that the peak is originated from Mu^0 in SiO_2.

Consequently, we were able to reconstruct an image of "Ag+SiO_2" sample as shown in Fig. 8 by visualizing the amplitudes on the nine areas in Fig. 7.

5 Summary, future works

In the present research, we developed a new detector set that has the spatial resolution and enables tracking positrons and successfully reconstructed the image of "Ag+SiO_2" sample by observing amplitudes of asymmetry for TF-μSR time spectra at each area in the sample. This means that we succeeded in distinguishing a metal and an insulator. Besides, this result suggests that it is possible to construct an image of a sample in which the distribution of compositions is unknown as long as there are differences in magnetic properties among the compositions. By the way, in fact, we measured the meteorite in experiments and the data is under analysis. We would like to increase statistics within the limited beamtime and improve the spatial resolution and analysis technique. To do so, we first have to improve the efficiency of our fiber trackers. It is only 40% for each fiber tracker on average so far because of the loss of light output due to connections between plastic scintillating fibers and optical fibers. We are expecting that if it rises to 80%, the overall efficiency will increase by an order of magnitude larger. Also, the development of a new data acquisition system would have an impact on it. The beam intensity we can utilize now is only 10% of the one used in typical μSR experiments due to the long dead time for data acquisition. Taking these two factors into account, the overall efficiency might become two orders of magnitude larger. Also, adding a position resolution to Muon counter could elevate this research as well. We can directly track μ^+ beam trajectories back with it and know where each μ^+ stops in the sample. By comparing the result obtained by it to the one acquired by fiber trackers, the spatial resolution would be better. In experiments, we measured many samples such as a granite, a meteorite, and even a shrimp as an organic sample. So we are going to proceed to the data analysis of them.

Ultimately, we are aiming to apply this research to other research techniques. For instance, the combination with muonic X-ray analysis hopefully makes it possible to identify the atom inside the sample very precisely. Moreover, we are exploring the application of this research in other fields such as medicine, astronomy, and so on.

Acknowledgements.

This work was supported by the Osaka University Research Activities 2022.

This work was supported by the Scholarship of Graduate School of Science of Osaka University for Overseas Research Activities 2022.

This work was supported by Fundamental Electronics Research Institute (FERI), Osaka Electro-Communication University (OECU) and JSPS Kakenhi Grant Number JP22H00110.

Declarations

Data availability Data are available from corresponding authors upon reasonable request.

Material availability Materials are available from corresponding authors upon reasonable request.

References

[1] Stephen J. Blundell, Roberto De Renti, Tom Lancaster, Francis L. Pratt, “Muon Spectroscopy - An Introduction”, OXFORD UNIVERSITY PRESS (2022)

[2] N. Kaplan et al.: Non-resonalt zeugmatograpy with muons (μSI) and radioactive isotopes. Hyperfine Interactions **87**, 1031-1041 (1994)

[3] Kuraray Co., Ltd., “Plastic Scintillating Fibers” https://www.kuraray.com/uploads/5a717515df6f5/PR0150_psf01.pdf (2023)

[4] Hamamatsu Photonics, “MPPC (Multi-Pixel Photon Counter) arrays S13361-3050 series”, https://www.hamamatsu.com/content/dam/hamamatsu-photonics/sites/documents/99_SALES_LIBRARY/ssd/s13361-3050_series_kapd1054e.pdf (2023)

[5] Y. Mizoi et al.: Application of β-*NMR* to Spectroscopy and Imaging. VIETNAM CONFERENCE ON NUCLEAR SCIENCE AND TECHNOLOGY-15, 302-306 (2023)

[6] Y. Mizoi et al.: β-*MRI*: new imaging device utilizing β-*NMR*. Interactions 245, 20 (2024)

[7] G. Takayama et al., "Evaluation of Image Resolution of Muon Spin Imaging", To be published in Interactions (2024)

[8] Centre for Molecular and Materials Science, TRIUMF, "Centre for Molecular and Materials Science, TRIUMF", https://cmms.triumf.ca (2023)

[9] TRIUMF, "TRIUMF Canada's particle accelerator centre", https://triumf.ca (2023)

[10] J. H. Brewer et al.: Delayed muonium formation in quartz. Physica B 239-240, 425-427 (2000)

[11] CERN, "ROOT Data Analysis Framework", https://root.cern